5300 Rcd
Guthrie

NRL Report 5977

5307 HP
5308 SJS

Retain

The Interpretation of Infrared Radiation from the Sea in Terms of its Boundary Layer

M. F. M. Osborne
Solid State Division

September 16, 1963

U.S. NAVAL RESEARCH LABORATORY
Washington, D.C.

CONTENTS

Abstract 1
Problem Status 1
Authorization 1

INTRODUCTION 1

THE OCEAN MODEL 2

THE HEAT EQUATION 4

INTERPRETATION OF THE HEAT BALANCE EQUATION 7

THE EFFECT OF VELOCITY VARIATIONS ON THE BOUNDARY LAYER 8

SOME EXPECTED TEMPERATURE PATTERNS 12

SUMMARY AND SOME THEORETICAL PROBLEMS 15

SOME POSSIBLE EXPERIMENTS 15

REFERENCES 17

APPENDIX A — Simplified Derivation of the Boundary Layer Thickness Ratio at the Water/Air Interface 18

APPENDIX B — Derivation of Derivatives of δ_w and δ_w/δ_a 19

The Interpretation of Infrared Radiation from the Sea in Terms of its Boundary Layer

M.F.M. Osborne
Solid State Division

By writing down the heat balance due to radiation, conduction, and evaporation at the sea surface, one can express the radiation temperature of the sea surface as a linear function with known coefficients of two variables: the water boundary layer thickness δ_w, and the ratio of water to air boundary layer thickness δ_w/δ_a. Under the assumption that these two variables can be described by laminar flow for short distance (< 10 cm) and small intervals (< 1 sec), one can derive the conditions for optimum observation of detailed structure in the sea surface temperature. These are clear sky, dry air, and especially an appreciable wind. Calculations were made of the small changes in the radiation temperature of the sea produced by mean air velocity changes of 1 cm/sec and mean water velocity changes of 1 mm/sec. A number of predictions were made concerning the temperature patterns to be observed around known velocity patterns in the air and water. The signs of the temperature fluctuations around some patterns may be reversed depending upon whether radiation or evaporation is dominant. Much experimentation is necessary to check and enlarge the conclusions. For example, slicks would generally be expected to be cold patches, even though they may have properties (such as decreasing the evaporation rate) which raise the surface temperature, and studies of slicks would be a good test of the theory.

INTRODUCTION

In this report we are trying to answer the following question, given a sequence in time or position of infrared radiation observations from areas of the sea surface, what precisely are we looking at? It is our thesis that what we "see" as "information" in such data are the *variations* in the boundary layer thickness δ_w of the water surface. To a lesser extent we see variations in the ratio $\delta = \delta_w/\delta_a$, the ratio of the water boundary layer thickness to that of the air. This conclusion is based on a consolidation of the work of widely separated workers. Ramdas and Raman (1) in India showed the existence of water and air thermal boundary layers in the laboratory and their variation with wind velocity. Ewing and MacAllister (2) in California and Ball (3) in Australia showed similar phenomena on a real ocean. Lock (4) in England gave a theory for the velocity dependence of the boundary layers. In what follows we attempt to unite the conclusions of these workers into a single coherent formula suitable for the interpretation of infrared radiation from the sea surface.

NRL Problem N03-01; Project RUDC-4-B-000/652-1/5031-01-00; Task 231-1. This is a final report on one phase of the problem; work on the other phases is continuing.

To begin with first principles: A radiometer puts out a signal in millivolts as a function of time, which is recorded on a paper x-y recorder. This signal in millivolts is normally converted either into an equivalent temperature of the patch of sea seen in the radiometer aperture, or to watts/cm^2-steradian radiated and reflected from this patch. Strictly speaking, either conversion implies a calibration of the radiometer by viewing a blackened can of warm water, plus the assumption that the can radiates in accordance with Planck's law. The calibration signal in millivolts is a measure of the temperature (or radiation) difference between the can of water and the sensitive element of the radiometer. In applying such a calibration to data from the sea surface, there may well be corrections due to reflection from the sea, to absorption and emission by the air between the radiometer and the sea, or to other causes. In what follows, we are going to assume that such corrections have been made, and speak of an observed radiation temperature of the sea surface, given by the radiometer.

We now ask, what physically determines that radiation temperature, and its variation in time or position on the sea? To do this we have to compute the heat balance between the sea surface and

its surroundings: the water below, the air above, and the sky.

THE OCEAN MODEL

Let us assume, afterward justifying our assumption, the following model (Fig. 1) of the sea and air, for which we can compute the energy balance:

1. A "sky" radiation temperature

$T_s = T(y = +\infty) = 293° - 50° = 243°K$ for a clear sky

$= 293° - 20° = 273°K$ for an overcast sky.

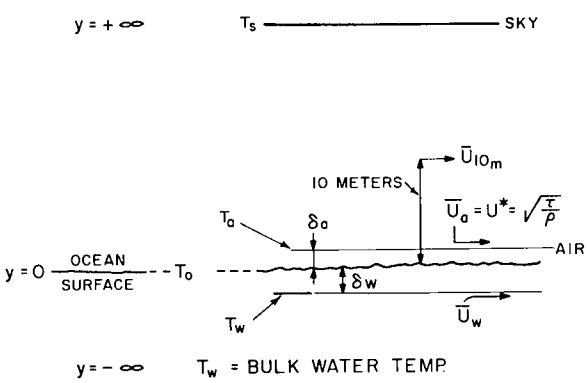

Fig. 1 — The atmosphere and ocean model

These sky temperatures correspond to a flux from the sky of 1/2 to 3/4 that from the sea surface, considered as a blackbody (5). Strictly speaking, to take into account the observed properties of sky radiation, one should qualify the definition of sky temperature to mean "as measured on a wavelength band at the atmospheric window of 10 microns." The reason for this qualification is that at neighboring wavelengths, 4.4, 6, and 15μ, the heavy absorption bands of CO_2 and H_2O make T_s close to the air temperature T_a in the neighborhood of the radiometer.

2. An air temperature T_a measured just above the air boundary layer at the water-sea interface. This air temperature we assume to be within the range $T_0 \pm 3°$, where T_0 is the water surface temperature.

3. An air boundary layer at the sea surface of thickness $\delta_a \approx 0.3$ to 0.1 cm (see Fig. 2). Within this air boundary layer, processes of viscosity (momentum transfer) are laminar; correspondingly, heat conduction and diffusion of water vapor are molecular. Above it, we suppose that the effective viscosity, heat conduction, and diffusion coefficients are much larger (effectively infinitely larger) due to turbulent mixing. By this assumption of turbulent mixing we are then also supposing that the air temperature T_a is sensibly constant an indefinite distance above the boundary layer. By this we would understand a distance large compared to δ_a but still small compared to a distance large enough to contribute appreciably to radiation; i.e., the fact that $T_a \neq T_s$ is not a contradiction in principle, even though the sky is contributing atmospheric radiation (see remarks under assumption 1.)

4. Just outside the air boundary layer the mean air velocity is $\overline{U}_a$, which varies from 13 to 36 cm/sec. These wind velocity limits (at the sea surface) correspond to a measured mean wind velocity U_{10m} at a height of 10 meters above the sea of 5 to 14 knots, assuming turbulent momentum transfer outside the boundary layer. The numerical values just quoted for the mean $\overline{U}_a$ just outside the boundary layer, correspond to values of the stress velocity $U^* = \sqrt{\tau/\rho_a}$ quoted by Defant (6), where τ is the surface stress and ρ_a the air density. Our notation will be $U_a = \overline{U}_a \pm \sigma_{u_a}$, where the rms fluctuation $\pm\sigma_{u_a}$ may be either large or small compared to $\overline{U}_a$. We are interested in the effect of small changes $\Delta\overline{U}_a$ on the mean thicknesses of the boundary layers δ_a and δ_w. The boundary layer thickness range, 0.3 to 0.1 cm, corresponds to the above velocity limits for $\overline{U}_a$ and U_{10m} (see Fig. 2).

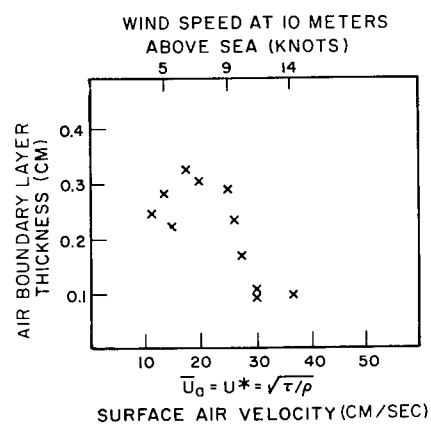

Fig. 2 — The air boundary layer thickness as a function of the mean air velocity just outside the air boundary layer. The scale at the top is the mean wind speed at a distance 10 meters above the sea surface. Data from Defant (6).

5. At the water-air interface the relative humidity of the air is 100 percent. Just outside the air boundary layer, it is between 0 and 100 percent. We assume the evaporation rate for the sea is determined by the rate of molecular diffusion across the air boundary layer. This assumption, with the above values of δ_a and $U^* = \overline{U}_a$, is just that used to represent the observed evaporation rates given by Defant (6).

6. At the surface of the ocean the water temperature is T_0, as observed by the radiometer. It is *this* temperature we wish also to compute, or more precisely, the difference between T_0 and the temperature of the water at some greater depth $T(y=-\infty)=T_w$.

7. Just as in the air, there is in the water surface a layer of thickness $\delta_w \approx 0.1$ cm, across which process of momentum and heat transfer occur molecularly, i.e., without turbulence (2, 3).

8. Just below the water boundary layer the horizontal velocity of the water is U_w. Our notation, as before, is $U_w = \overline{U}_w \pm \sigma_{u_w}$, and we are interested in the effect of small changes $\Delta\overline{U}_w$ on the thicknesses of the boundary layers δ_a and δ_w.

9. The temperature of the water just below the water boundary layer is $T(y=-\infty) = T_w$ and is constant for an indefinite distance downward. This is essentially the same assumption as that made for air. In our numerical work we shall assume $T_w = 293°K$ throughout. Thus, we are also assuming that turbulence (convection) raises the effective thermal conductivity of the water outside the boundary layer to a value large compared to its molecular thermal conductivity. There may well be upwelling currents bringing water near the surface of slightly different temperature, but we are going to ignore (for the moment) this effect on our heat balance equation.

The experimental evidence (2, 3) for the existence of air and water boundary layers on a real ocean seems unquestionable. However, it might be well to review the theoretical arguments for their existence, since we are going to use formulas for laminar flow in both air and water at the surface, even in the presence of a surface agitated by wind and waves, and this is not an obviously valid procedure.

In the presence of a rigid boundary in turbulent flow, the argument for the existence of microscopic laminar boundary layer inside a turbulent boundary layer is as follows (7): Both theoretically and experimentally the mean velocity gradient normal to the surface $\partial\overline{u}/\partial y$ for turbulent flow approaches infinity at the rigid boundary. Since this implies literally an infinite stress $\mu(\partial\overline{u}/\partial y)$, which is actually observed as finite, the condition of turbulence must break down at very small distances from the rigid boundary. Simply put, a rigid boundary must suppress the turbulent fluctuations close to it.

The question we ask here is, does this argument apply to a nonrigid boundary such as an agitated air-water interface? It probably does, within the context we shall use it, for the following reason. Consider the approximate expression for the growth in thickness of the boundary layer on a rigid plate started in motion from rest at time $t = 0$; this is $\delta \approx \sqrt{\nu t}$, where ν is the kinematic viscosity. Equivalently, for flow at velocity V past a plate of length l, $t = l/V$ is the time a fluid particle is in interaction with the plate, and so

$$\delta \approx \sqrt{\nu l/V}.$$

Solving for the times or distances of interaction, we find

$$t_{int} = \delta^2/\nu;\ l_{int} = \delta^2 V/\nu = t_{int}V. \qquad (1)$$

Now we are discussing boundary layers in air of thickness $\delta_a \approx 0.3$ to 0.1 cm, and velocities $\overline{U}_a$ from 13 to 36 cm/sec. In water we shall assume we are interested in mean velocities $\overline{U}_w$ from 0.1 cm/sec to 10 cm/sec and $\delta_w \approx 0.1$ cm. Thus the range of observed boundary layer thicknesses and velocities of interest give upper limits to the time t and length l over which our boundaries are asked to be effectively stationary, so that the concepts of boundary layer growth at rigid boundary might be applicable. If these times and lengths are small, or at most comparable to the wavelengths and periods of water agitation, then we might hope that stationary-boundary laminar flow concepts would have a certain validity.

For a boundary layer in air of thickness 0.3 cm, Eq. (1) gives

$$t_{int} = 0.3^2/0.15 = 0.6 \text{ sec}$$

and, since $\overline{U}_a \approx 13$ cm/sec corresponds to $\delta_a \approx 0.3$ cm (see Fig. 2),

$$l_{int} = t_{int}V = t_{int}\overline{U}_a = 0.6(13) = 8 \text{ cm}.$$

For a boundary layer in air of thickness 0.1 cm, Eq. (1) gives

$$t_{int} = 0.1^2/0.15 = 0.07 \text{ sec}$$

and

$$l_{int} = 0.07(36) = 2.5 \text{ cm}.$$

For a boundary layer in water of thickness 0.1 cm, Eq. (1) gives

$$t_{int} = 0.1^2/0.01 = 1 \text{ sec}$$

and $l_{int} = 0.1$ cm for $U_w = 0.1$ cm/sec, and $l_{int} = 10$ cm for $U_w = 10$ cm/sec.

Looking at these interaction times and lengths we see that, certainly for the air, and to a lesser extent the water, the treatment of the water/air interface as rigid (nonbending, not nonshearing) is somewhat justified for short intervals of distance and time. From a deductive viewpoint one might prefer to say that the momentary development of the boundary layer thickness was broken up after intervals of approximately 1 sec or less and distances of approximately 10 cm or less by the irregular wave motion, and that the actual mean boundary layer thickness developed was determined by some kind of an average determined by the spectral distribution of the particle velocities and wavelengths in air and water at the surface.

The time intervals calculated above have a second interpretation which is important. Taking the simpler case of air first, these time intervals also represent the time required for an air layer of thickness δ_a suddenly subjected to a thermal disturbance (abrupt change of temperature at one of its boundaries) to reach a new condition of steady-state heat flow. This second interpretation follows from the fact that, close to the boundary, momentum flow is determined by the equation

$$\frac{\partial u}{\partial t} = \nu \frac{\partial^2 u}{\delta y^2}$$

and thermal flux by

$$\frac{\partial T}{\partial t} = \frac{\kappa}{\rho c}\frac{\partial^2 T}{\partial y^2} = \kappa \frac{\partial^2 T}{\partial y^2}.$$

The ratio of the controlling parameters ν/κ (the Prandtl number Pr) is of order 1 (0.7 for air), so that thermal and momentum boundary layers more or less coincide.

The case of water is not quite so simple. For water, the Prandtl number is 6.2 ($T = 290°$K). It can be shown that in circumstances where both momentum and heat flux occur, the thermal and momentum boundary layer thicknesses are in the ratio $(1/\text{Pr})^{1/3}$ (Ref. 8, p. 627). Thus, for water the thermal boundary layer is only about 55 percent as thick as the velocity boundary layer. The boundary layer measurements for water quoted under assumption 7 of our ocean model were for a thermal boundary layer in the ocean. The thickness was estimated from the time constant for its establishment and the required gradient.

For simplicity in what follows below, we are going to use the velocity determined boundary layer thickness also as the thickness of the thermal boundary layer. Actually, very little is known experimentally about the thickness of the thermal or velocity water boundary layers in the ocean, and our numerical results are intended only to represent signs and orders of magnitude.

THE HEAT BALANCE EQUATION

Let us now write down the heat balance, corresponding to Fig. 1, to the ocean surface (plus sign) and from the ocean surface (minus sign) at temperature T_0.

1. The energy radiated to the ocean from the sky is σT_s^4 cal/cm²-sec, where $\sigma = 1.35 \times 10^{-12}$ cal/cm²-sec-°C⁴, Stefan-Boltzmann's constant.

2. The energy radiated to the sky from the ocean surface is $-\sigma T_0^4$.

Terms 3, 4, and 5 below express the heat flux as proportional to the gradient of temperature or water vapor density.

3. The conduction from the ocean surface to the air is $-k_a(T_0 - T_a)/\delta_a$, where $k_a = 5.7 \times 10^{-5}$ cal/cm-sec-°C and δ_a is the thickness of the air boundary layer in centimeters.

4. The transfer from the ocean surface by evaporation is

$$-\frac{\omega L\ (\rho_{sat} - \rho_{water\ vapor})}{\delta_a} = \frac{\omega L\ (R.H. - 1)\ \rho_{sat}}{\delta_a}$$

where ω is the molecular coefficient of diffusion, 0.239 cm/sec² for water vapor in air at 18° C; L

is the latent heat of water, 590 cal/gm; ρ_{sat} is the saturation density of water vapor, 17×10^{-6} g/cm^3, over (fresh) water at $T = 20°C$; $\rho_{water\ vapor}$ is the density of water vapor in air just outside δ_a, in g/cm^3; and $R.H.$ is the relative humidity (as a decimal), $\rho_{water\ vapor}/\rho_{sat}$.

5. The conduction into the water from ocean surface is $-k_w(T_0 - T_w)/\delta_w$, where $k_w = 1.3 \times 10^{-3}$ cal/cm-sec-°C, $T_w = 293°K$, and δ_w is, strictly, the thermal boundary layer thickness in centimeters.

The heat balance in the steady state is the sum of these five terms equated to zero;

$$+ \sigma T_s^4 - \sigma T_0^4 - k_a \frac{(T_0 - T_a)}{\delta_a} + \frac{\omega L (R.H. - 1)\ \rho_{sat}}{\delta_a} - k_w \frac{(T_0 - T_w)}{\delta_w} = 0. \quad (2)$$

Equation (2) is then an implicit equation for determining T_0 in the steady state, given the values of parameters and temperatures which appear. If we are interested in determining T_0 to say 0.1°C, this is a very complicated and troublesome implicit function for T_0 indeed. To this degree of accuracy all the parameters L, $\rho_{water\ vapor}$, ρ_{sat}, k_a, and k_w are themselves appreciable varying functions of the temperature in the boundary layers, not to mention the parameters δ_w and δ_a, which depend on viscosity (itself dependent on temperature), and other variables too, in a complicated and unknown way. Fortunately, our interests allow a considerably simpler procedure. We are interested, not directly in T_0 to 0.1°C, but in changes in T_0 of this order of magnitude as we move to different positions and times on the surface of the sea. We can also be reasonably certain that T_o, in first approximation will be T_w, the temperature of the bulk ocean beneath the water boundary layer.

We can, therefore, express $T_0 = T_w$ plus small corrections as follows: The difference $T_0 - T_w$ is considerably smaller than the difference $T_0 - T_s$, or $T_w - T_s$. So we shall expand Eq. (2) around T_w, keeping only the linear terms, even though linear terms alone are not sufficient to represent T_0 to an accuracy of 0.1°C:

$$\sigma T_s^4 = \sigma T_w^4 + 4\sigma T_w^3\ (T_s - T_w) + \ldots$$

$$\sigma T_0^4 = \sigma T_w^4 + 4\sigma T_w^3\ (T_0 - T_w) + \ldots.$$

Substituting these two expansions into Eq. (2) and defining $4\ \sigma T_w^3 = \alpha$, Eq. (2) becomes

$$\alpha\ (T_s - T_0) + k_a \frac{(T_a - T_0)}{\delta_a} + k_w \frac{(T_w - T_0)}{\delta_w} + \frac{\omega L \rho_{sat}\ (R.H. - 1)}{\delta_a} = 0$$

or

$$T_0 \left(\alpha + \frac{k_a}{\delta_a} + \frac{k_w}{\delta_w}\right) = \alpha T_s + \frac{k_a}{\delta_a} T_a + \frac{\omega L \rho_{sat}\ (R.H. - 1)}{\delta_a} + \frac{k_w}{\delta_w} T_w. \quad (3)$$

To proceed with further simplification we note, using our numerical estimates for δ_a and δ_w and appropriate values for the other physical constants which appear, that the terms in k_w/δ_w are by far the largest terms on both the right and left side, confirming incidentally that which was physically obvious, $T_0 \approx T_w$. Dividing on both sides by k_w/δ_w and transposing we have

$$T_0 = \frac{T_w + T_s \frac{\alpha \delta_w}{k_w} + \frac{k_a}{k_w} T_a \frac{\delta_w}{\delta_a} + \frac{\omega L \rho_{sat}\ (R.H. - 1)}{k_w} \frac{\delta_w}{\delta \alpha}}{\left(1 + \frac{\alpha \delta_w}{k_w} + \frac{k_a}{k_w} \frac{\delta_w}{\delta_w}\right)}. \quad (4)$$

Finally, in order to focus attention on dimensionless parameter ratios which are either near unity, or small compared to unity, and again keeping only the first order of small quantities in expanding the denominator, we have

$$T_0 = T_w + \underbrace{T_w \left(\frac{T_a}{T_w} - 1\right) \frac{k_a \delta_w}{\kappa_w \delta_a}}_{(A)} + \underbrace{T_w \left(\frac{T_s}{T_w} - 1\right) \frac{\alpha \delta_w}{k_w}}_{(B)} + \underbrace{T_w \frac{\omega L \rho_{set}}{k_w} \frac{(R.H. - 1)}{T_w} \frac{\delta_w}{\delta_a}}_{(C)}. \quad (5)$$

The correction terms A, B, and C to T_w as a measure of T_0 we shall refer to as the conduction,

radiation, and evaporation terms. Some typical values are given in Table 1.

In the form given in Eq. (5) we can see rather clearly how the deviations of the radiation temperature of the surface T_0 from the bulk water temperature T_w arise. Evidently a promising term for appreciable deviation is the second one, B, which depends on the considerable deviation of the sky temperature T_s from T_w, and on the thickness of the (thermal) water boundary layer. If the sky is overcast, or a heavy fog lies close to the sea, this term becomes relatively less important. It also gets negligible (or even changes sign) in the polar regions in summer, or in daylight. The effect of air temperature deviation from T_w is given by the first term, A. We can see it is likely to be small, except under rather special conditions (polar regions, or a sudden blast of hot or cold air over the sea). The effect of the evaporation rate, as altered by small surface contaminants can be read from the third term. Here ρ_{sat} $(R.H.-1)$ is best written directly as $\rho_{water\ vapor} - \rho_{sat}$, since it is the saturation vapor density ρ_{sat} (or its equivalent in pressure) which is more directly affected by contaminants. We mention that the salinity of the sea diminishes ρ_{sat} by 2 percent from its fresh water value, as an indication of how large such an effect might be.

Mathematically we have been slightly inconsistent in not expanding ρ_{sat}, k_w, L, etc., as linear functions of temperature T_0, since for changes in T_w of say 5°C, T_0 is affected to more than 0.1°C in the correction term. The reason we have not done so is that most of the changes in T_0 due to changes in T_w are already contained in the T_w term itself. Thus in passing over a cold or

TABLE 1

The Upper Limit in Magnitude of the Conduction (A), Radiation (B), and Evaporation (C) Terms for $T_0 - T_w$ in Eq. (5)

Term in Eq. (5)	Value of Pertinent Factor in the Term	Upper Limit of the Term (°C)			
		$\delta_w/\delta_a = 1.5$ $0 < \lambda < 0.027$ $\delta_a = 0.3$ cm $\delta_w = 0.45$ cm $U^* < 20$ cm/sec $U_{10m} < 9$ knots $\overline{U}_w < \lambda U^*$ $\overline{U}_w < 0.6$ cm/sec	$\delta_w/\delta_a = 1.5$ $0 < \lambda < 0.027$ $\delta_a = 0.1$ cm $\delta_w = 0.15$ cm $U^* > 20$ cm/sec $U_{10m} > 9$ knots $\overline{U}_w < \lambda U^*$ $\overline{U}_w < 0.6$ cm/sec	$\delta_w/\delta_a = 0.18$ $\lambda > 1$ $\delta_a = 0.3$ cm $\delta_w = 0.053$cm $U^* < 20$ cm/sec $U_{10m} < 9$ knots $\overline{U}_w > \lambda U^*$ $\overline{U}_w > 20$ cm/sec	$\delta_w/\delta_a = 0.18$ $\lambda > 1$ $\delta_a = 0.1$ cm $\delta_w = 0.018$ cm $U^* > 20$ cm/sec $U_{10m} > 9$ knots $\overline{U}_w > \lambda U^*$ $\overline{U}_w > 20$ cm/sec
A Conduction	$T_a = T_w \pm 3$°C	± 0.19	± 0.19	± 0.02	± 0.02
B Radiation	$T_s = 243$°K (clear)	-2.1	-0.7	-0.25	-0.085
	$T_s = 273$°K	-0.93	-0.31	-0.10	-0.033
C Evaporation	0% relative humidity	-2.8	-2.8	-0.3	-0.3
	75% relative humidity	-0.7	-0.7	-0.085	-0.085

warm current in the ocean, most of the observed change in T_0 is that due to T_w directly.

We should mention here an alternative way of looking at our model, which will emphasize just what information is contained in the first term, T_w for T_0, as opposed to the correction terms which depend on δ_w and δ_w/δ_a. We have described the ocean, and also the atmosphere, as two media through which (excluding radiation) a constant flux of energy F occurs, proportional to a gradient of temperature, or water vapor density:

$$F \propto K\Delta\theta/\Delta y,\ \theta = \text{temperature or } \rho_{water\ vapor}. \quad (6)$$

The exchange coefficient K may be a function of position and time, but in any event is greater than or equal to the molecular value which obtains in the absence of any stirring or turbulence. We have approximated our real ocean and atmosphere by assigning the minimum value to the boundary layers, and implied $K \to \infty$ and $\Delta\theta/\Delta y \to 0$ elsewhere.

A more refined theory (2, 6) and experimental evidence would show that actually $\theta \approx \theta_0 \log (z/z_0)$ (for $z > z_0$), where z is the distance from the interface, and z_0 is of the order of the boundary layer thickness. Equivalently $K \approx K_0\ (z/z_0)$ (for $z > z_0$). Our oversimplified model throws the burden of representing temperature fluctuations on the boundary layer thickness fluctuations. One could in many cases put the burden on variations in the factor K and leave the boundary layer thickness a constant; the distinction is perhaps mathematical in representation rather than physical.

An example will make the two points of view clear. Consider a pot of thick pudding on the stove, which is stirred to prevent scorching (i.e., to cool) the bottom of the pot. One can say either the stirring increases the effective K of the pudding, which cools the bottom of the pot, or that the stirring thins the thermal laminar boundary layer at the bottom of the pot. This also increases the heat flux, or cools the pot.

An analogous situation in the ocean would be the stirring of a patch of water by a subsurface school of fish. Such a patch would appear as a hot patch on the sea. It could be described by giving either a locally increased K, or a locally decreased water boundary layer thickness. From Eq. (5), a decrease of δ_w implies an increase of T_0, if we ignore term A. In what follows, we are going to use the boundary-layer point of view, though there may well be cases (as for time-dependent flux) where this is not the best point of view to adopt.

INTERPRETATION OF THE HEAT BALANCE EQUATION

Let us, therefore, concentrate on those changes in T_0 not directly influenced by T_w, i.e., the A, B, and C terms of Eq. (5). It will then be seen that the greatest uncertainty lies in the factors δ_w and δ_w/δ_a. All other parameters appearing are certainly known or measurable to a few percent. The temperature correction $T_w - T_0$ is then a linear function with known coefficients of the unknowns δ_w and δ_w/δ_a. In order to see just how large these correction terms are, we have given in Table 1 (and in Tables 3 and 4) some typical values of these corrections for various plausible combinations of parameters. We have also given values for the parameter $\lambda = \bar{U}_w/\bar{U}_a$, the ratio of velocity of water to air; concerning this parameter and the associated values of δ_w/δ_a we shall have more to say later. The values most likely to obtain on the open sea are a relative humidity of 75 percent, a sky either clear (T_s = 243°K) or overcast (T_s = 273°K), and $\lambda \approx 0$ (no steady current in the sea), or $\lambda > 1$ (a condition given by a strong water current and light winds). $\lambda > 1$ can also be interpreted to mean that fluctuations σ_{U_w} in the horizontal water particle velocity U_w (or wave motion) are larger than the mean *wind* velocity $\bar{U}_a$. The values for the air boundary layer thickness, and associated wind velocities $\bar{U}_a = U^*$, and U_{10m} (10 meters above the sea) are taken from Fig. 2. The water boundary layer thicknesses are determined from the air boundary layer thickness and Lock's (4) theoretical values of the ratio δ_w/δ_a. For $\lambda < 1$ the values of δ_w agree, in order of magnitude, with the few observations (2, 3) (see also Table 6).

The magnitude of the correction terms listed in Table 1 can be regarded as absolute upper limits to the fluctuation in T_0 which might appear in our infrared data. They can easily be used to estimate the change in T_0 when one of the parameters is slightly changed. For example, with $\lambda \approx 0$ in term B, if for some unspecified reason a 20-percent decrease occurs in the water boundary layer δ_w (and also δ_a, so that δ_w/δ_a remains constant), then (for wind speeds greater than 9 knots)

an increase is implied in the sea radiation temperature T_0 of 0.14°C for a clear sky (20 percent of 0.7°C) and 0.06°C on a cloudy one. On the other hand if δ_a increases by 20 percent but δ_w remains fixed, so the ratio δ_w/δ_a declines, then from term C for $\lambda \approx 0$, for 75 percent relative humidity, T_0 increases by 0.14°C, independently of whether the sky is clear or cloudy. In both the above examples, if the air temperature differed from the water temperature by ± 3°C, there would be additional ± 0.04°C change in T_0 for $\lambda \approx 0$ or ± 0.004°C for $\lambda > 1$. These latter changes are of course negligible and suggest that air temperature changes, in their effect on changes of T_0, the sea surface temperature, are relatively small.

As a third example, imagine a surface contaminant, of material which decreases the saturation vapor pressure (equivalently, ρ_{sat}) by 2.5 percent. This decreases the evaporation rate by 10 percent (at 75 percent relative humidity) and increases the surface temperature T_0 for $\lambda = 0$ by 0.07°C (1/40 × 2.8°C, term C), independently of whether the sky is clear or overcast, and also independent of the actual relative humidity (i.e., value of $\rho_{water\ vapor}$). For $\lambda > 1$, the increase is 0.008°C, a negligible amount.

Evidently there are many possible combinations of small disturbances which might be evaluated by adding effects according to Table 1. Nevertheless, even without a knowledge of the differentials of the terms in Eq. (5) and Table 1, we can specify the favorable and unfavorable condition for the general observation of sea surface structure. Foggy or overcast condition, high humidity, small air-water temperature difference, and large average values of λ (very small or no wind, but somewhat agitated sea) are unfavorable; the converse of all these, favorable. But one should note that the combination of small λ and large U_w (including the rms fluctuation σ_{u_w}) normally go together, but there is not always a strictly 1-to-1 relation between sea agitation and the mean wind.

THE EFFECT OF VELOCITY VARIATIONS ON THE BOUNDARY LAYER

We wish now to focus attention on the factors of greatest uncertainty, δ_w and δ_w/δ_a. How are these affected, particularly as regards the velocities U_a and U_w? Since our information is contained in the fluctuation of T_0, we are really asking about the differentials $(\partial T_0/\partial U_w)\Delta U_w$ and $(\partial T_0/\partial U_a)\Delta U_a$. To compute these, we need the derivatives of δ_w and δ_w/δ_a, since all the other parameters in Eq. (5) are practically constant.

Unfortunately, not too much is known experimentally (over the ocean) about δ_a as a function of $\overline{U}_a$ except that it decreases with increasing $\overline{U}_a$; that is, $d\delta_a/d\overline{U}_a$ is negative (Fig. 2). This is not of much help. Our formula tells us we need to know the derivatives $[d/d(U_w \text{ or } U_a)](\delta_w/\delta_a)$, and especially $\partial\delta_w/\partial(U_w \text{ or } U_a)$. There are no data whatsoever on these points.

Fortunately there is a theory for the laminar behavior of δ_w and δ_w/δ_a. This theory we may use, with caution, and within the limitations of short distance and small time mentioned in the Introduction. This theory may at least tell us what to look for concerning these derivatives, and the order of magnitude of the effects to be expected.

Lock (4) solves the following idealized boundary layer problem. Two "semi-infinite" fluids of densities ρ_a, ρ_w, viscosities μ_a, μ_w, and velocities U_a, U_w (which, if not zero, are in the *same* direction) are brought into dynamical contact on the $y = 0$ plane for all $x > 0$. He then evaluates the flow pattern for all y, $x > 0$, and in particular the boundary layer thickness in both fluids as a function of x. This is no wave generation; the stability he examines in a subsequent paper. His results are as follows (see Appendix A): The ratio $\xi = (\delta_w/\delta_a)/(\mu_w/\mu_a) = \delta/\mu$, the ratio of the thicknesses of the boundary layers in the water and the air divided by the ratio of the viscosities, is independent of x and is given as function of the velocity ratio $\lambda = U_w/U_a$ by the implicit function

$$\xi^2 = \frac{1}{\rho\mu}\,\frac{(2\xi + 1 + \lambda)}{[\xi(1+\lambda) + 2\lambda]} \tag{7}$$

in which, by definition, $\rho = \rho_w/\rho_a$ and $\mu = \mu_w/\mu_a$. Lock gives as approximate solutions when $\rho\mu$ is large ($\rho\mu \approx 5 \times 10^4$ for a water/air interface)

$$\xi = \left(\frac{1+\lambda}{2\lambda\rho\mu}\right)^{1/2}, \quad \lambda > 0 \tag{8}$$

$$\xi = 1/(\rho\mu)^{1/3}, \quad \lambda = 0. \tag{9}$$

The distinction between the two cases $\lambda = 0$ and $\lambda > 0$ tells us something rather interesting about the derivatives of δ_w/δ_a and hence the differentials $(\partial T_0/\partial U_a)\Delta\overline{U}_a$, $(\partial T_0/\partial U_w)\Delta\overline{U}_w$ whose maximum possible values appear in Table 1. Equation (8) for $\lambda > 0$, taken literally, indicates that both

$\xi \to \infty$ and $d\xi/d\lambda \to \infty$ as $\lambda \to 0$, yet at $\lambda = 0$, $\xi = (\rho\mu)^{-1/3}$, independent of λ. Hence for λ somewhere close to zero, exactly how close being determined by the implicit relation Eq. (7), this infinite behavior must be modified. For differentials of T_0, whose largest possible values appear in Table 1, this means that most of the possible changes there tabulated may occur in relatively small ranges of λ, and hence in small ranges of $\bar{U}_w$ and $\bar{U}_a$.

This leads one to look for what might be called amplification (as a temperature fluctuation) in a critical range of λ near zero of quite small changes in the velocity of the water and air. As we shall see, this suspicion turns out to be correct. This critical range occurs in the small range from $\lambda = 0$ to $\lambda = 1/(\rho\mu)^{1/3}$.

Let us write Eq. (5) in the form

$$T_0 = T_w(1 + A'\delta_w/\delta_a + B'\delta_w + C'\delta_w/\delta_a) \quad (10)$$

where A', B', and C' are given in cgs units in Table 2. Table 1 gives the corresponding values of $T_0 - T_w$ in degrees centigrade. The differential of Eq. (10) is

$$\left(\frac{\partial T_0}{\partial U_a}\right)_{U_w const} \Delta U_a = T_w A' \frac{\delta_w}{\delta_a}\left[\frac{\partial(log(\delta_w/\delta_a))}{\partial U_a}\right]_{U_w const}$$

$$+ T_w B' \delta_w \left[\frac{1}{2}\frac{\partial}{\partial U_a} log(\delta_w)^2\right]_{U_w const}$$

$$+ T_w C' \frac{\delta_w}{\delta_a}\left[\frac{\partial}{\partial U_a} log\,(\delta_w)\right]_{U_w const} \quad (11)$$

and similarly for $(\partial T_0/\partial U_w)_{U_a\ const}$. The reason for expressing these derivatives in terms of the derivative of the logarithm, is that the observed temperature changes

$$\Delta T_0 = \left(\frac{\partial T_0}{\partial U_w}\right)_{U_a const} \Delta U_w \ or \ \left(\frac{\partial T_0}{\partial U_a}\right)_{U_w const} \Delta U_a$$

can then be obtained by direct multiplication of the maximum temperature change $T_w A'$ (δ_w/δ_a), $T_w B' \delta_w$, etc., given in Table 1 or in Eq. (5) or (10) by the logarithmic differential. In the case of the δ_w term in Eq. (11) the use of a square canceled by 1/2 makes for easier algebra (Appendix B). One must be careful to ensure that the changes $\Delta\bar{U}_a$, $\Delta\bar{U}_w$ and the statistical fluctuations σ_{u_a}, σ_{u_w} are not so large as to violate the conditions of applicability of the formulas, which are restricted to certain values of λ.

TABLE 2
Numerical Coefficients to Determine the Maximum Change in the Sea Surface Temperature T_0 as Given by Eq. (10)

Coefficient	Condition	Value of Coefficient
A'	$T_a - T_w = \pm 3°C$	$\pm 0.44 \times 10^{-3}$ (dimensionless)
B'	Clear sky	-1.6×10^{-2} cm^{-1}
	Overcast	-0.7×10^{-2} cm^{-1}
C'	0% *R.H.*	-0.63×10^{-2} (dimensionless)
	75% *R.H.*	-0.16×10^{-2} (dimensionless)

Tables 3 and 4 give values of the logarithmic derivatives of δ_w/δ_a and δ_w for various values of the parameter λ, using Lock's formulas. Appendix B gives the details of the evaluation. It should be particularly noted that the derivatives

$$\left(\frac{\partial T_0}{\partial U_w}\right)_{U_a const} and \left(\frac{\partial T_0}{\partial U_a}\right)_{U_w const}$$

are not the same as

$$\left(\frac{\partial T_0}{\partial U_w}\right)_{\lambda\ const} and \left(\frac{\partial T_0}{\partial U_a}\right)_{\lambda\ const}.$$

Nevertheless, our tables are arranged according to the parameter λ, since this is the parameter which controls the magnitude of ΔT_0.

Tables 5 and 6 give the calculated temperature change in sea surface temperature T_0, ΔT_0 for the radiation and evaporation terms B and C, for assumed changes ΔU_a = 1 cm/sec and ΔU_w = 1 mm/sec, together with an estimate of the implied maximum fluctuations $\pm\sigma_{u_a}$, $\pm\sigma_{u_w}$ for the calculation to be valid. These velocity changes have been chosen small for convenience. Larger velocity changes give proportionally larger temperature changes.

TABLE 3

Derivatives of log $\delta_w/\delta_a \equiv log\ \delta$, for Various Values of λ; Computed from Eq. (7)

$$\frac{1}{(\delta_w/\delta_a)}\frac{\partial(\delta_w/\delta_a)}{\partial U}=\frac{\mu_w}{\mu_a}\frac{1}{(\delta_w/\delta_a)}\frac{\partial\xi}{\partial U}=\frac{\mu_w}{\mu_a}\left(\frac{\partial\lambda}{\partial\xi}\right)^{-1}\frac{1}{(\delta_w/\delta_a)}\frac{\partial\lambda}{\partial U},\ \text{where } U=U_a \text{ or } U_w.$$

$$\epsilon^{1/3}=\left(\frac{\rho_w}{\rho_a}\frac{\mu_w}{\mu_a}\right)^{-1/3}=(\rho\mu)^{-1/3}=0.027.$$

Value of λ	$\xi \equiv \frac{\delta_w/\delta_a}{\mu_w/\mu_a}$	$\frac{\delta_w}{\delta_a}$	$T_wC'\delta_w/\delta_a$ at 75% r.h. (°C)	$\left(\frac{\partial\ log\ \delta_w/\delta_a}{\partial U_a}\right)_{U_w\ const}$	$\left(\frac{\partial\ log\ \delta_w/\delta_a}{\partial U_w}\right)_{U_a\ const}$
0 *to* 0.027	$\epsilon^{1/3}$	1.5	−0.7	$+\frac{2}{3}\frac{\lambda}{U_a\epsilon^{1/3}}$	$-\frac{2}{3}\frac{}{U_a\epsilon^{1/3}}$
1/7	$2\epsilon^{1/2}$	0.5	−0.24	$+\frac{7}{16U_a}$	$-\frac{49}{16U_a}$
1	$\epsilon^{1/2}$	0.25	−0.12	$+\frac{1}{4U_a}$	$-\frac{1}{4U_w}$
>>1	$(\epsilon/2)^{1/2}$	0.18	−0.085	$+\frac{1}{2U_w}=\frac{1}{2\lambda U_a}$	$-\frac{1}{2\lambda U_w}=-\frac{1}{2}\frac{U_a}{U_w^2}$

TABLE 4

The Derivatives of log $(\delta_w)^2 = 2\ log\ \delta_w$ for Various Values of λ. $\epsilon = (1/\rho\mu) = 0.21 \times 10^{-4}$.

λ	$T_wB'\delta_w$ (clear sky) (°C)		$\left(\frac{\partial\ log\ \delta_w^2}{\partial U_a}\right)_{U_w\ const}$	$\left(\frac{\partial\ log\ \delta_w^2}{\partial U_w}\right)_{U_a\ const}$
	$\delta_a = 0.3\ cm$	$\delta_a = 0.1\ cm$		
0 *to* 0.027	−2.1	−0.7	$-\frac{1}{U_a}$	$-\frac{1.3}{\epsilon^{1/3}U_a}$
1/7	−0.7	−0.22	$-\frac{1}{U_a}2.5\epsilon^{1/2}$	$-\frac{7}{U_a}$
1	−0.35	−0.11	$-\frac{1}{U_a}\epsilon^{1/2}$	$-\frac{1}{U_a}$
>>1	−0.25	−0.078	$-\frac{1}{4U_w}\sqrt{\frac{\epsilon}{2}}$	$-\frac{1}{U_w}$

There are a number of assumptions in Tables 5 and 6 which must be mentioned. For the term $T_wB'\delta_w$ (radiation term) we have assumed the favorable case of a clear sky. For the case of an overcast sky the entry under this term should be reduced by approximately 1/2 (see Table 2). For the term $T_wC'\delta_w/\delta_a$ (evaporation term) we have assumed a relative humidity of 75 percent as typical of the value on a real ocean. The tabulated values would become zero for 100 percent humidity, be 1/5 as large for 95 percent humidity, and be 4 times as large for dry air.

Since the only boundary layer thickness for which we have any real knowledge is δ_a, we have used two cases, δ_a = 0.3 cm and δ_a = 0.1 cm, corresponding to wind speeds outside the boundary layer greater or less than 20 cm/sec, or winds at a height of 10 meters above the sea greater or

TABLE 5
Calculated Changes in the Radiation Temperature T_0 of the Sea for an Increase $\Delta\overline{U}_a = 1$ cm/sec in the Mean Air Speed $\overline{U}_a = 20$ cm/sec

λ	σ_{u_a} (cm/sec)	$\overline{U}_w$ (cm/sec)	σ_{u_w} (cm/sec)	δ_w (cm)	(*Clear Sky*) $\Delta T_0 = T_w B' \frac{\partial \delta_w}{\partial U_a} \Delta \overline{U}_a$ (°C)	$\frac{\delta_w}{\delta_a} = \xi\mu$	(75% *Relative Humidity*) $\Delta T_0 = T_w C' \frac{\partial(\delta_w/\delta_a)}{\partial U_a} \Delta \overline{U}_a$ (°C)
0 *to* 0.027	±5	0 *to* 0.54	<±0.27	0.45 0.15	0.052 0.017	1.5	0 *to* −0.023
1/7	±5	3	<±1	0.15 0.05	0.002 0.0007	0.5	−0.0053
1	±5	20	±5	0.075 0.025	0.0004 0.00013	0.25	−0.0014
>>1	±20	50	~±20	0.053 0.018	0.2×10^{-5} 0.7×10^{-6}	0.18	0 *to* −0.00085

TABLE 6
Calculated Changes in the Radiation Temperature T_0 of the Sea for an Increase $\Delta\overline{U}_w = 1$ mm/sec in the Mean Water Velocity. $\overline{U}_a = 20$ cm/sec

λ	σ_{u_a} (cm/sec)	$\overline{U}_w$ (cm/sec)	σ_{u_w} (cm/sec)	δ_w (cm)	(*Clear Sky*) $\Delta T_0 = T_w B' \frac{\partial \delta_w}{\partial U_w} \Delta \overline{U}_w$ (°C)	$\frac{\delta_w}{\delta_a}$	(75% *Relative Humidity*) $\Delta T_0 = T_w C' \frac{\partial(\delta_w/\delta_a)}{\partial U_w} \Delta \overline{U}_w$ (°C)
0 *to* 0.027	±5	0 *to* 0.54	≤±0.27	0.45 0.15	0.26 0.08	1.5	0.09
1/7	±5	3	<±1	0.15 0.05	0.012 0.0004	0.5	0.0035
1	±5	20	<±7	0.075 0.025	0.0009 0.0003	0.25	0.00015
>>1	±20	>50	~±20	0.053 0.018	0.00025 0.00008	0.18	0.00003

less than 9 knots (see Fig. 2). Once we have these values for δ_a, we compute the *theoretical* values for δ_w/δ_a for the various values of λ and hence also we obtain the values of δ_w. These computed values of δ_w agree in order of magnitude with the few observations for λ near zero (3, 4).

The derivatives of δ_w and δ_w/δ_a are computed from Lock's theory for different values of λ. The experimental parameter controlling the theory is δ_a, but this affects only the B term (in δ_w), since the ratio δ_w/δ_a is completely determined by theory, given the assumed values of λ. The assumed fluctuations σ_{u_w} and σ_{u_a} are simply given as approximate upper limits which should not be appreciably exceeded for the theoretical derivatives, with constant λ, to be approximately valid. The temperature changes in Tables 5 and 6 are in general below the range of measurement for the arbitrary small velocity changes assumed. Bigger velocity changes give proportionately bigger temperature changes.

Examination of the entries in Tables 5 and 6 confirm our original suspicion that for small systematic surface velocity changes in either air or water, the ratio $\lambda = U_w/U_a$ must be small to give detectable signals in ΔT_0. However, if our

minimum detectable signal is set at 0.1°C, and the smallest systematic changes of interest as $\Delta\bar{U}_w \approx 0.1$ cm/sec and $\Delta\bar{U}_a \approx 1$ cm/sec, it will be seen that appreciable signals, $\Delta T_0 > 0.1$, are given over a limited range of conditions for λ near zero. For a real ocean it seems likely that in the neighborhood of $\lambda = 0$, the statistical fluctuations due to σ_{u_w} will cut down, for example, the radiation term B of 0.26°C for 1 mm/sec water velocity change for $\delta_w = 0.45$ cm. The evaporation term C is barely detectable for 75 percent humidity (0.09°C at $\lambda = 0$) and dies off with increasing λ.

We can now specify what the conditions with respect to wind and sea state are likely to be for optimum observations, *i.e.*, the most information in our infrared tracing due to small changes of $\bar{U}_w$ or $\bar{U}_a$. Let us begin by imagining a dead calm (in the air) with the sea somewhat realistically agitated by disturbances a distance away (swell) or a previous condition of wind. The mean λ, and its fluctuation σ_λ, is certainly $>>1$, since $\lambda = U_w/U_a$ and we have specified $\bar{U}_a = 0$, $\sigma_{u_a} = 0$. If we now imagine a slight breeze to spring up, the effective λ must certainly decline, and our signals

$$\Delta T_0 = \frac{\partial T_0}{\partial U_w}\,\Delta U_w \textit{ and } \frac{\partial T_0}{\partial U_a}\,\Delta U_a$$

will increase in strength. If air velocity continues to increase, we cannot expect λ to decline and our signal strengths to increase indefinitely. The sea state must ultimately become more and more agitated with increasing wind velocity, or λ, and certainly σ_λ will stop decreasing due to the present wind. There must be then an optimum value for the wind velocity such that the ratios $\sigma_{u_w}/\bar{U}_w$, $\sigma_{u_a}/\bar{U}_a$, and $\sigma_\lambda/\lambda = \sqrt{\sigma_{u_a}^2/U_a^2 + \sigma_{u_w}^2/U_w^2}$ are as small as possible. $\sigma_{u_w}/\bar{U}_w$, and $\sigma_{u_a}/\bar{U}_a$ cannot be expected to decrease indefinitely with increasing wind speed. The effective minimum, say of $\sigma_{u_w}/\bar{U}_w$, for optimum signal from say, the radiation term B with respect to wind speed may be a relatively broad one. In such case, the conditions for observation for this term will be good over a fairly wide range of wind speeds.

SOME EXPECTED TEMPERATURE PATTERNS

Let us now see what our theory tells us to expect about the configuration of surface temperature T_0 around some known water and wind velocity patterns in the sea. Table 7 gives the signs of the temperature derivatives from the terms B and C for positive increments $\Delta\bar{U}_a$ and $\Delta\bar{U}_w$. Both $\bar{U}_w$ and $\bar{U}_a$ are supposed parallel and in the same direction. It will be noted that three of the derivatives are positive and one is negative, so that there may be circumstances where the terms B and C predict opposite effects. The A term (conduction) is usually small, and we have neglected it. In any event, the A term will reinforce the C term (evaporation) when the air is colder than the sea and will diminish the C term if the air is warmer than the sea. This statement is valid only if the relative humidity is held constant, but over a real ocean, the sea-air temperature difference and relative humidity may well be strongly correlated.

We take signs from Table 7 by specifying B as dominant when the sky is clear and the air damp,

TABLE 7

Signs of the Temperature Increment to the Radiation Temperature of the Sea T_0 Caused by Positive Increments $\Delta\bar{U}_a$ and $\Delta\bar{U}_w$ to the Mean Air and Water Velocities. The signs for B term are for $T_s < T_w$, a condition which usually holds for both night and day, if we understand by T_w the restricted definition for radiation at the $10-\mu$ atmospheric window.

Increment	Sign of the Increment	
	Radiation Term B in δ_w	Evaporation Term C in δ_w/δ_a
$(\partial/\partial U_w)\ \Delta\bar{U}_w$	+ (hotter)	+ (hotter)
$(\partial/\partial U_a)\ \Delta\bar{U}_a$	+ (hotter)	− (colder)

making the evaporation term C small; correspondingly the term C dominates when the sky is heavily overcast and the wind dry. Since there is no way of knowing which will actually dominate without giving explicit conditions, we can also say that for those cases where the two terms are of opposite sign, the effect will be stronger in one case (clear and damp) than in the other (overcast and dry). For simplicity we have indicated a reversal, which may not actually occur. Meteorologically, the conditions "clear and damp" or "overcast and dry" are somewhat contradictory, so that clear-cut cases where either B or C alone dominate will be somewhat rare.

The first hypothetical case is that of a ship at anchor (or small island or dock pier) in no water current with a wind blowing with velocity $\bar{U}_a$. The wind flow around an obstacle is known to be decelerated at points into and away from the wind, and accelerated at the widest point of the obstacle. So we assign $\bar{U}_a - \Delta\bar{U}_a$ at points fore and aft, and $\bar{U}_a + \Delta\bar{U}_a$ abeam. Term B dominant and term C dominant give opposite temperature patterns, as shown in Fig. 3a. Exactly how much the "hot" and "cold" temperatures in Fig. 3 deviate from the surrounding undisturbed temperature can be estimated from calculations similar to those given in Tables 5 and 6 and the way the air velocity disturbance falls off around an obstacle. If d is the diameter of the obstacle, and r is the distance of the point of observation from it, the velocity disturbance dies off roughly as $(d/r)^3$.

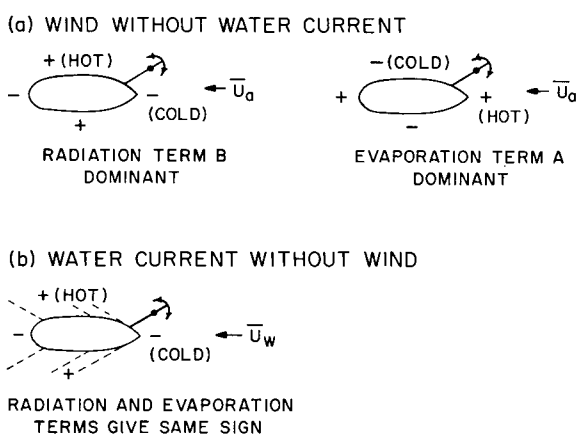

Fig. 3 — Temperature pattern (a) around a ship at anchor in a wind with no water current and (b) around a ship in a water current with no wind. The pattern in (b) is strengthened by a wind parallel to the water current.

The second configuration is that of a ship at anchor in a current (tide say) with no wind. In this case the corresponding effects of $\Delta\bar{U}_w$ in terms B and C agree in the sign of the effect, which is the same as for B dominant in Fig. 3a. Note that the effects for the "ship at anchor in a tide" configuration should be much more pronounced in a light breeze, air velocity greater than water current, $\lambda < 1$, than in a dead air calm, $\lambda >> 1$.

As a third example, we have given in Fig. 4a the velocity and presumed temperature pattern for a confined channel with a current where the depth, and hence mean velocity, is assumed greater in the middle than along the shoreline. For no wind the contrast is much less between center and shoreline than in the presence of a wind. For a fair breeze downstream, the center channel is hotter than the shoreline. The effect of shallow water in a confined channel with current is shown in Fig. 4b. Here a shallow or constriction compels the current to move more swiftly, and the shallow or constricted water is warmer. The effect is increased by the presence of wind (small λ).

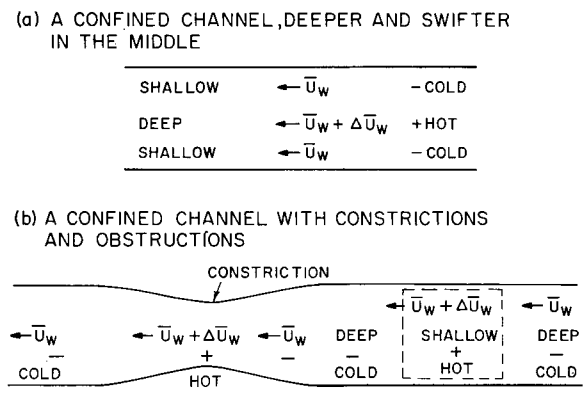

Fig. 4 — Temperature patterns for a channel: (a) no obstruction; (b) obstructions which increase the velocity

Figure 5 shows a case of shallow water in the absence of any *confined* current, say at the edge of the sea. If there is a tidal current, one can apply the argument for Fig. 4a to infer that the shallow water appears colder, especially in the presence of wind. In the absence of any current, one might argue (by ignoring wave effects) that the presence of a second boundary (the bottom) close to the surface, would tend to suppress turbulence. This decreases K (Eq. (6)), or equivalently increases the boundary layer thickness, and makes the shallow

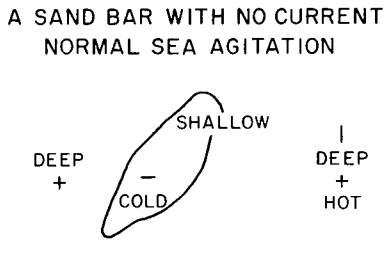

Fig. 5 – Temperature pattern around a sand bar with no water current

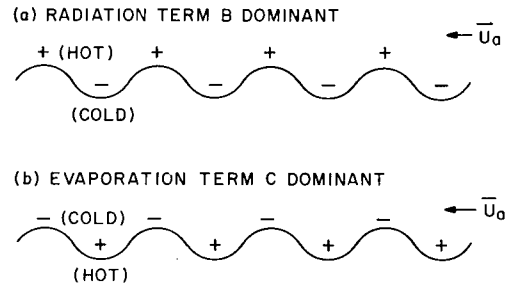

Fig. 6 – Temperature patterns given by wind over traveling waves

water colder. However, shallow water due to a sand bar, and shallow water due to rocks or reef might well be different. The former appears as a consequence of the absence of stirring; the latter may well be associated with increased turbulence, with opposite effects on the boundary layer thickness, or K.

However, these examples raise some questions which show the inadequacy of the theory. Lock's theory was developed for U_w and U_a both parallel, if not zero, but in these cases one can obviously imagine circumstances where U_w and U_a are opposite to each other, or at an angle. What happens then to the temperature pattern we are at a loss to state. The same difficulty applies to Fig. 3b for a ship at anchor in a current and nonparallel wind.

Presumably the effect of wind, after some time, would be to create a superficial current of depth much greater than the boundary layer, and in the direction of the wind, so that the conditions of Lock's problem would be superficially applicable. One might then add to this superficial current, small components proportional to the component of the undertow in the direction of the superficial wind and water current. The validity of this approach is open to question and would be best settled by experiment.

As our final example, more complex and yet more commonplace than any of the preceding ones, consider the case of a simple series of traveling waves, Fig. 6. These might be the Kelvin wake of a ship or the ground swell on the open sea. For the moment consider only the effect of the wind, U_a. We neglect momentarily the horizontal to and fro motion of the water particles in the surface. With this neglection, for zero wind, there is no thermal effect, one cannot distinguish troughs from crests. In the presence of a wind one might expect the wind velocity U_a to be slightly greater at the crests, and perhaps on the face of the wave toward the wind, than in the troughs and sheltered face. On this hypothesis, radiation B and evaporation C contribute oppositely (Fig. 6).

If we endeavor to add to this picture the complications introduced by the water motion, we are led into some difficulties. The actual path of the water particles in such waves is circular. Thus the maximum horizontal velocities are equal to the maximum vertical velocities. Table 8 gives some typical values. These velocities are in the direction of the wave propagation at the crest, and oppositely at the troughs. The magnitude of these velocities are small compared to the velocity of the wind, say at 10 meters (or even 1 meter), but they are certainly not always small compared to the wind velocity just outside the air boundary layer, which is of order $U^* \approx 10$ to 30 cm/sec (Fig. 2). Just how to take into account these fluctuating water velocities in this problem we do not know. Nor do we know how to distinguish the case of wind with or against the wave propagation

TABLE 8

Typical Maximum Horizontal Particle Velocity Amplitudes, for Water Surface Waves of Different Wavelengths. A constant ratio of trough-to-crest height/wavelength of 1/20 has been assumed (Ref. 6, Vol. II).

Phase Velocity (cm/sec)	Wavelength (cm)	Horizontal Maximum Particle Velocity (cm/sec)
23.2 (minimum)	1.73	3
46	13.6	8
92	55	15
186	220	31

direction. This question deserves more study, both theoretically and experimentally.

SUMMARY AND SOME THEORETICAL PROBLEMS

We can summarize the results of this report as follows. We have deliberately restricted our discussion of the infrared radiation from the sea to what might be called "structure" on an "isothermal in the horizontal direction" ocean. Within this restriction, the temperature picture of the ocean still presents considerable structure, which we have interpreted in terms of its theoretical "momentum" boundary layer, assuming that momentum and thermal boundary layers were proportional. Of especial interest is the importance of the air velocity in bringing out the details in the data, which depend primarily on the sky temperature and the relative humidity of the air immediately above the sea. But one should not forget that there are other elements in radiometric data from the sea we have not discussed. These are caused by variations in the transmission of the air over the sea, variation in its reflective coefficient, and obviously, departures from the conditions of isothermal in the horizontal direction.

There are a number of serious gaps in our discussion. First among these is the behavior of the boundary layer when water velocity and wind are in opposite directions, *i.e.*, $\lambda = U_w/U_a < 0$. This gap might be filled in by solving Lock's problem for an "aperature" of finite length, where water and air were in contact.

A second and perhaps more satisfactory way to fill the gap would be to evaluate the behavior of the boundary layer directly for a train of progressive waves. This would, we think, require solving the problem of waves at an interface, taking account of viscosity, relative velocity, and possibly also surface tension. Examination of the partial solution of this problem (9, 10) confirms Lock's conclusion that for $\lambda >> 1$, $\delta_w/\delta_a \approx 1/(\rho\mu)^{1/2}$. There is no indication that the behavior $\delta_w/\delta_a \approx 1/(\rho\mu)^{1/3}$ (for $\lambda = 0$) appears in these wave solutions. It would be important to confirm this $(\rho\mu)^{-1/3}$ behavior for the boundary layer ratio in the wave-type solutions, since this is the condition which Lock's theory indicates will give the largest observed temperature fluctuations. Availability of a complete wave-type solution for boundary layer thickness would simplify the problem of averaging over a sea-state spectrum, a question which we have not discussed adequately. It may well be that one would have to include in the equation of motion the full expression for the velocity derivative $du/dt = \partial u/\partial t + u\partial u/\partial x + v\partial u/\partial y$ (and similar terms in the temperature equation), which characterize Gerstner's waves (9). Only the last two terms are the ones which Lock uses ($u\partial u/\partial x$ and $v\partial u/\partial y$) rather than only the first one. Just the first term $\partial u/\partial t$ characterizes most linear wave problems.

The above is a rather formidable theoretical program, and in addition is deficient in that it does not include the effect of turbulence in the air, which may well be the controlling factor on the boundary layers.

SOME POSSIBLE EXPERIMENTS

We wish to describe here a number of possible laboratory and field experiments to check and enlarge on the conclusions we have drawn so far. Returning to our basic Eq. (5) we see that T_0 is, as we mentioned, a linear function in the two unknowns, δ_w and δ_w/δ_a. This suggests the following experimental technique for measuring these two unknowns under a variety of conditions, and at the same time checking on the overall validity of our assumptions. Figure 7 generalizes the experiment of Ramdas and Raman (1). It shows a tank or channel of water fitted with an artificial sky of variable temperature and with provisions for adjusting wind velocity, air temperature, relative humidity (evaporation rate), water velocity, and degree of agitation by waves. To measure δ_w one holds all other variables constant and plots the observed radiation temperature of water surface T_0 against the variable sky temperature T_s. The slope of such a plot gives directly the measured value of δ_w for the given condition. In a similar way the slope of a plot of radiation temperature against variable relative humidity (with $T_a = T_w$) gives the ratio δ_w/δ_a.

In the absence of an experimentally controlled velocity for the water, it is possible that the wind motion plus the boundaries of the tank would produce an unspecified and perhaps unrealistic (relative to the ocean) circulation in the tank. Thus we have shown arrangements for controlling the water and air velocities over the entire area. If the tank is square or if a long canal is used for the experiment, one could also examine the effect of

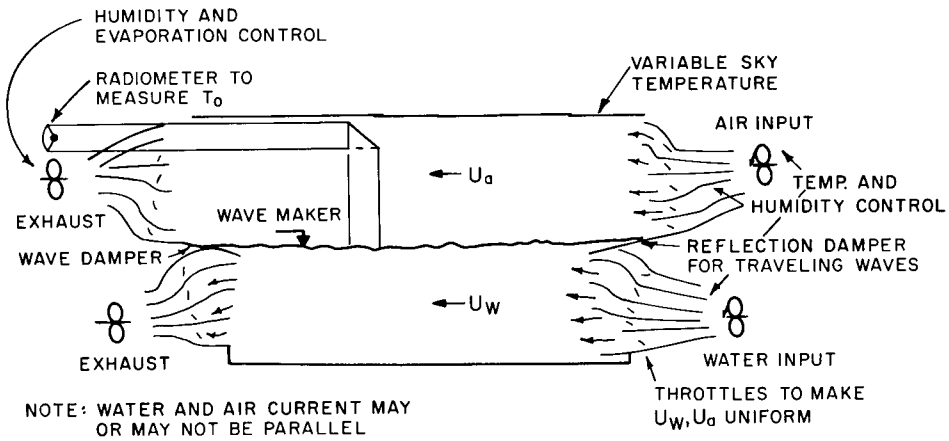

Fig. 7 — Radiometric measurement of δ_w and δ_w/δ_a

nonparallel wind and water velocities, a state of affairs we have not been able to describe theoretically. In particular, such experiments would be useful in analyzing the effect of a progressive wave train, the effects of which we were unable to predict in any convincing way, especially in the absence of wind.

The experiments described in Fig. 7 could also be reproduced in part over the ocean. One can imagine a heated canopy, or artificial sky, say 10 meters square, set up at the end of a dock on the open sea. Measurement of the sea surface temperature under this canopy (with a radiometer and deflecting mirror) could give a measure of δ_w alone for the ocean, just as in the laboratory experiment. Observation with a louvered canopy, or "partially overcast sky," might suffice to vary the effective sky temperature. If the laboratory experiments confirmed the general validity of Eq. (5), field data under a variety of conditions could be analyzed by least squares to obtain, simultaneously, mean values of δ_w/δ_a and δ_w.

There are other simple field experiments which would be helpful in directly explaining the signs of the various thermal terms contributing to ΔT_0, especially for the case of known wave patterns and velocities. One or two identical boats proceeding on paths such as to reverse signs of the wind and water particle velocity would be of interest in showing just what patterns give hot and cold for different conditions of wave slope and direction of the wind. Simultaneous optical data sufficient to unambiguously determine crest from trough would, of course, be necessary. The case of an auxiliary-powered sailboat would be particularly interesting, as then wind vs water wake could be compared. One could also compare the water wakes with momentum (sail-driven) as opposed to without momentum (engine-driven). This comparison could also be made with two identical boats, one towed with a long rope, the other self-powered.

A final simple experiment would be to put (or find) on the open sea, a stable slick of material which did not affect evaporation rate via ρ_{sat} but which did thicken the water boundary layer (11). Such a slick's temperature relative to its surroundings should change in a predictable way with the sky temperature and in general be a cold patch (Table 9, B, (2)).

A stable slick which decreased evaporation via ρ_s without affecting the water boundary layer δ_w would in contrast be a warm patch, altering in temperature with the humidity, but unaffected by the sky temperature (Table 9, C (3)).

Finally, a stable slick which did neither of the above but instead diminished the ripple height (via surface tension and surface viscosity) would presumably diminish δ_a. Such a slick would be a cold patch (insofar as evaporation term C is concerned, Table 9, C (1)). It should alter in its temperature T_0 with humidity and air temperature and be unaffected by the sky temperature.

In practice, natural or synthetic slicks do not have the pleasant property of only changing one of the above variables at a time. The net effect of a given slick is a combination of all the above effects

TABLE 9
Effects of Slicks on Sea Surface Temperature

Term in the Expression for T_0	Effect on Term and Hence on T_0		
	(1) Decrease δ_a (surface tension plus surface viscosity smoothes the water)	(2) Increase δ_w (surface convection suppressed)	(3) Decrease ρ_s (decrease evaporation)
A. Conduction Term (depends on T_a)	+ (hotter) when $T_a > T_w$ − (colder) when $T_a < T_w$	+ (hotter) when $T_a > T_w$ − (colder) when $T_a < T_w$	0
B. Radiation Term (depends on T_s)	0	− (colder)	0
C. Evaporation Term (depends on relative humidity)	− (colder)	− (colder)	+ (hotter)

as summarized from Eq. (5) in Table 9. Generally speaking it will be seen that the effect of a slick is to diminish T_0 (cold slick), an effect which is augmented if $T_a < T_w$. The tendency of a slick to be cold is less pronounced if the slick happens to be one which decreases the evaporation rate.

The above conclusion that slicks tend to be *cold*, relative to the surrounding sea (B and C, cols. 1 and 2, Table 9) is specifically restricted to the radiation *surface* temperature T_0. *Underneath* a slick, the temperature of the bulk *water*, T_w, may well be *warmer*, relative to the surrounding sea water. The reason for this paradoxical state of affairs is that some slicks tend to have a blanketing effect (cols 2 and 3, Table 9). This, plus the fact that the exchange coefficient K is large and finite, rather than infinite, as we have assumed, tends to make the water *beneath* the boundary layer at a slick a little warmer.

It would be a good test of the theory to put simultaneously on the open sea a number of different slick-forming materials. Their temperatures should be ordered according to their physical properties as measured in the laboratory, and in accordance with the prediction from Eq. (5) and Table 9.

REFERENCES

1. Ramdas, L.A., and Raman, P.K., Indian Acad. of Sci. Proc. A23:127 (1946)
2. Ewing, G., and McAllister, E.D., Science 131:1374 (1960)
3. Ball, F.K., Australian J. Phys. 7:649 (1954)
4. Lock, R.C., Quarterly J. Mechanics and Appl. Math. IV:42 (1951)
5. Brunt, D., "Physical and Dynamical Meterorology," 2nd ed, Cambridge:University Press, 1939, p. 139
6. Defant, A., "Physical Oceanography," New York:Pergamon, Vol. I, 1961, p. 229
7. Prandtl, L., and Tietjens, O.G., "Applied Hydro- and Aeromechanics," New York:McGraw Hill, 1934, pp. 78-80
8. Goldstein, S., editor "Modern Developments in Fluid Dynamics," Oxford:Clarendon Press, Vols. I, II, 1938
9. Lamb, H., "Hydrodynamics," 6th ed., Cambridge:University Press, 1932 pp. 370-373, 417-421, 627
10. Harrison, W.W., Proc. Lond. Math. Soc. (2), VI:396 (1908)
11. Jarvis, N.L., "The Effect of Monomolecular Films on Surface Temperature and Convective Motion on an Air-Water Interface," NRL Report 5726, Jan. 9, 1962

APPENDIX A

SIMPLIFIED DERIVATION OF THE BOUNDARY LAYER THICKNESS RATIO AT THE WATER/AIR INTERFACE

In this appendix we wish to give a brief and heuristic derivation of the two limiting forms of Lock's result for the ratio of the boundary layer thicknesses. For the reasons given in the text, we assume that boundary layers will exist in the two fluids. We let the velocity in the undisturbed air be U_a, the velocity of both liquids at the interface be u_0 (continuity of velocity at the interface), and the undisturbed velocity of the water be U_w. Then continuity of the surface stress requires approximately $\mu_a = (\partial U_a/\partial y) = \mu_w(\partial U_w/\partial y)$, or approximately, in terms of our boundary layer hypothesis,

$$\mu_a \frac{U_a - u_0}{\delta_a} = \mu_w \frac{u_0 - U_w}{\delta_w}. \tag{A1}$$

Solved for u_0, this gives

$$u_0 = \frac{U_w + U_a \dfrac{\delta_w}{\delta_a}\dfrac{\mu_a}{\mu_w}}{1 + \dfrac{\delta_w}{\delta_a}\dfrac{\mu_a}{\mu_w}} \tag{A2}$$

a result given by Lock.

For the individual boundary layer thicknesses we appeal to the general and approximate theory of boundary layers. Here there are two possibilities:

1. A flat plate, started from rest at $t = 0$, causes a boundary layer to grow to a thickness

$$\delta \approx \sqrt{\nu t} \text{ at time } t.$$

If we imagine water and air layers of indefinite extent but of differing velocities brought into contact at $t = 0$, we have

$$\delta_a \approx \sqrt{\nu_a t} \text{ and } \delta_w \approx \sqrt{\nu_w t}.$$

From this we have

$$\frac{\delta_w}{\delta_a} = \sqrt{\frac{\nu_w}{\nu_a}} = \sqrt{\frac{\mu_w}{\mu_a}\frac{\rho_a}{\rho_w}} = \frac{\mu}{(\rho\mu)^{1/2}} \tag{A3}$$

which is the limiting form $\left(\text{neglecting } \sqrt{2}\right)$ of Lock's result for $\lambda = (U_w/U_a) >> 1$.

2. If we imagine two layers of water and air of finite length l to be brought into horizontal contact at $t = 0$, then the time of interaction of particles is $l/(u_0 - U_w)$ for the water and $l/(U_a - u_0)$ for the air. In these time intervals the layers are distorted by their own lengths l, or demolished. So we have

$$\delta_a \approx \sqrt{\frac{\nu_a l}{U_a - u_0}}$$

$$\delta_w \approx \sqrt{\frac{\nu_a l}{u_0 - U_w}}.$$

The ratio of these is

$$\frac{\delta_a}{\delta_w} = \sqrt{\frac{\nu_a}{\nu_w}\frac{u_0 - U_w}{U_a - u_0}}. \tag{A4}$$

Substituting the ratio $(u_0 - U_w)/(U_a - u_0)$ from the expression for the continuity of the surface stress, Eq. (A1), we ultimately obtain

$$\frac{\delta_w}{\delta_a} \quad \frac{\mu_w}{\mu_a}\frac{1}{\left(\dfrac{\rho_w}{\rho_a}\dfrac{\mu_w}{\mu_a}\right)^{1/3}} = \frac{\mu}{(\rho\mu)^{1/3}} \tag{A5}$$

which is Lock's result for $\lambda = (U_w/U_a) = 0$. Lock's exact result (Eq. (7)) is essentially an interpolation formula between these two limiting cases.

APPENDIX B

DERIVATION OF DERIVATIVES OF δ_w AND δ_w/δ_a

In this appendix we want to derive the analytical results which form the background of Tables 3, and 4. These contain the derivatives of δ_w and δ_w/δ_a with respect to U_w and U_a. For the derivatives of δ_w/δ_a we have, imagining Eq. (7) to be solved for $\xi = \xi(\lambda)$,

$$\frac{\partial(\delta_w/\delta_a)}{\partial U_w \text{ or } \partial U_a} = \frac{\mu_w}{\mu_a}\frac{\partial \xi}{\partial \lambda}\frac{\partial \lambda}{\partial U_w \text{ or } \partial U_a}.$$

From this we see that the critical quantity is $\partial\xi/\partial\lambda$. To get this, it will be easiest to solve Eq. (7) explicitly for $\lambda = \lambda(\xi)$ and compute $\partial\xi/\partial\lambda = (\partial\lambda/\partial\xi)^{-1}$. We also define $1/\rho\mu = \epsilon$ as a small quantity. We obtain

$$\lambda = \frac{-(\xi^3 - 2\epsilon\xi - \epsilon)}{(\xi^3 + 2\xi^2 - \epsilon)}. \tag{B1}$$

The controlling parameter in λ and $d\lambda/d\xi$ is evidently ϵ. The largeness or smallness of ξ with respect to ϵ or some power of ϵ will be critical in determining $\lambda = \lambda(\xi)$ and $d\lambda/d\xi$.

From Eq. (B1) we find

$$\frac{d\lambda}{d\xi} = \frac{-(2\xi^4 + 4\xi^3 + 4\epsilon\xi^2 + 4\xi\epsilon + 2\epsilon^2)}{(\xi^3 + 2\xi^2 - \epsilon)^2}. \tag{B2}$$

From Eq. (B1) one can construct the following tabulation in order of decreasing value of ξ:

$\xi = +\infty$	$\lambda = -1$	
$\xi = +\epsilon^{1/3}$	$\lambda = 0$	Physical range of interest, Eqs. (8) and (9)
$\xi = \sqrt{\epsilon/2} + 0$	$\lambda = +\infty$	
$\xi = \sqrt{\epsilon/2} - 0$	$\lambda = -\infty$	
$\xi = 0$	$\lambda = -1$	
$\xi = \sqrt{\epsilon/2} + 0$	$\lambda = -\infty$	
$\xi = -\sqrt{\epsilon/2} - 0$	$\lambda = +\infty$	
$\xi = -1$	$\lambda = +1$	
$\xi = -2 + 0$	$\lambda = +\infty$	
$\xi = -2 - 0$	$\lambda = -\infty$	
$\xi = -\infty$	$\lambda = -1.$	

Lock restricts the discussion of his solution to the branch between $\lambda = 0$ to $+\infty$ for positive values of ξ, since only in this range is the solution physically a function only of $x > 0$. Goldstein* gives an illuminating commentary on the erratic behavior of the boundary layer thickness computed by momentum theory, which the above table of λ vs ξ illustrates. Table B1 gives values for ξ, λ, and $d\lambda/d\xi$ for the range of physical interest.

TABLE B1

The Physical Range of Interest of the Boundary Layer Ratio $\xi = (\delta_w/\delta_a/\mu_w/\mu_a) = \delta/\mu$ as a Function of the Velocity Ratio $\lambda = U_w/U_a$. $\epsilon \equiv (\rho_w/\rho_a)^{-1}(\mu_w/\mu_a)^{-1} = (\rho\mu)^{-1}$.

λ	ξ	$d\lambda/d\xi$
0 *to* $\epsilon^{2/3}$	$\epsilon^{1/3}$	$-3/2$
1/7	$2\epsilon^{1/2}$	$-(8/49)\epsilon^{-1/2}$
1	$\epsilon^{1/2}$	$-4\epsilon^{-1/2}$
>>1	$\sqrt{\epsilon/2}$	$-(\sqrt{2/\epsilon})\ 2\lambda^2$

*S. Goldstein, editor, "Modern Developments in Fluid Dynamics," Oxford:Clarendon Press, Vol. I, p. 134, 1938

From Table B1 we can compute

$$\left(\frac{\partial\left(\frac{\delta_w}{\delta_a}\right)}{\partial U_a}\right)_{U_w\,const} = \frac{\mu_w}{\mu_a}\left(\frac{d\xi}{d\lambda}\right)\frac{\partial\lambda}{\partial U_a}$$

$$= \frac{\mu_w}{\mu_a}\left(\frac{d\xi}{d\lambda}\right)\left(-\frac{U_w}{U_a^2}\right) \tag{B3}$$

and similiarly

$$\left(\frac{\partial\left(\frac{\delta_w}{\delta_a}\right)}{\partial U_w}\right)_{U_a\,const} = \frac{\mu_w}{\mu_a}\left(\frac{d\xi}{d\lambda}\right)\frac{\partial\lambda}{\partial U_w} = \frac{\mu_w}{\mu_a}\left(\frac{d\xi}{d\lambda}\right)\frac{1}{U_a} \tag{B4}$$

to obtain the values quoted in Table 3 and the last column of Table 5 of the text.

To obtain the derivatives $\partial\delta_w/\partial U_a$ and $\partial\delta_w/\partial U_w$ we use either of the expressions from Lock:

$$\delta_w^2 = \frac{2\nu_2 x}{U_w}\left(\frac{1+\xi}{2+\xi+\xi/\lambda}\right) \tag{B5}$$

or

$$\delta_w^2 = \frac{2\nu_2 x}{U_a}\left(\frac{1+\xi}{2\lambda+\xi\lambda+\xi}\right). \tag{B6}$$

Equation (B5) will be used to compute $\partial\delta_w^2/\partial U_a$, and Eq. (B6) to compute $\partial\delta_w^2/\partial U_w$. Equation (B5) gives

$$\frac{\partial\delta_w^2}{\partial U_a} = \frac{2\nu_2 x}{U_w}\frac{\partial}{\partial\lambda}\left(\frac{1+\xi}{2+\xi+\xi/\lambda}\right)\frac{\partial\lambda}{\partial U_a}$$

$$= \frac{2\nu_2 x}{U_w}\frac{\frac{\partial\xi}{\partial\lambda}(\lambda^2-\lambda)+\xi+\xi^2}{(2\lambda+\xi\lambda+\xi)^2}\frac{\partial\lambda}{\partial U_a}. \tag{B7}$$

Equation (B6) gives

$$\frac{\partial\delta_w^2}{\partial U_w} = \frac{2\nu_2 x}{U_a}\frac{\partial}{\partial\lambda}\left(\frac{1+\xi}{2\lambda+\lambda\xi+\xi}\right)\frac{\partial\lambda}{\partial U_w}$$

$$= \frac{2\nu_2 x}{U_a}\frac{\left(\frac{\partial\xi}{\partial\lambda}(\lambda-1)-\xi^2-3\xi-2\right)}{(2\lambda+\lambda\xi+\xi)^2}\frac{\partial\lambda}{\partial U_w}. \tag{B8}$$

Using Table B1 for values of ξ and $d\xi/d\lambda$ as a function of λ gives the results quoted in Table 4 and the sixth column of Table 6.